Defence Science Journal, Vol. 53, No. 1, January 2003, pp. 87-94

Avalanche Initiaition Mechanism – A Finite-element Approach

S. Senthil and P. Mahajan

Indian Institute of Technology Delhi, New Delhi – 110 016

ABSTRACT

The Himalayas, the longest chain of mountains in the world, experiences extensive snowfall and avalanche activity during winter. Some of these areas are densely populated, and death and destruction on large scale due to avalanche activity has been reported in these areas. One of the ways of reducing the loss of life and material due to avalanches is through prediction of avalanches. An understanding of weather forecasting, terrain, and avalanche initiation mechanism is a prerequisite for avalanche prediction. In the present paper mathematical modelling of avalanche initiation mechanism has been discussed.

Keywords: Avalanche, super-weak zones, debonding, avalanche prediction, avalanche initiation mechanism, finite-element method, mathematical modelling

1. INTRODUCTION

A snowpack on the slope is rarely homogenous and consists of a number of layers of varying microstructure and properties. Depending on the weather conditions that these layers experience during their formation, or later, these can have varying strength. A weak layer embedded in the layered snowpack reduces the strength of the whole snowpack. The weak layer normally has super-weak zones (cracks) which act as stress raisers. Also, it does not form a good bond with the snow layers between which it is sandwiched. Under sustained shear loads due to gravity load or overloads due to fresh snowfall, the propagation of crack becomes the main reason for slab failure and an avalanche to occur.

It is now commonly assumed in literature that shear failure of snow followed by tensile crown failure, is the main mechanism of slab avalanche initiation[1,2]. Many studies[1,2] exist that model a snowpack as a continuum with a discontinuity, such as a crack. They also report large stress concentration close to the discontinuity. A review of slab avalanche release has recently been published by Schweizer[3]. Based on simple statical calculations, he reports the length of the discontinuity to be between 0.1 m to 8 m depending on the tensile strength of snow[3]. These discontinuities have, however, not been observed in the field conditions and Schweizer suggests the use of statistical approach to study avalanche initiation. The weak zone approach along with fracture mechanics has been used by McClung[4] and Bader and Salm[5]. These authors have attempted to tackle the problem using two different approaches. McClung applied a model developed by Palmer and Rice[6] for the growth of shear band in an over consolidated clay mass. The approach specifies that a shear band is initiated at the stress concentration in the weak layer; a slow strain softening

Received 24 October 2002

at the tip of the crack follows, until a critical length is reached, where upon the crack propagates rapidly. The Palmer and Rice model is able to predict a number of features of snow slab failure. Bader and Salm introduced a super-weak zone within the weak zone. Using finite-element method, they calculated stresses, strains, and strain rates in a snowpack. If at tip of super-weak zone strain rates equal the critical value for ductile fracture propagation, a fracture propagates. The speed of propagation is calculated assuming a constant shear stress and strain rate value over the length of influence, which is the distance from the end of the super-weak zone to a point where shear stresses reach 105 per cent of the undisturbed value. Brittle failure starts if the crack length is large enough for the strain rates at crack tip to exceed brittle failure.In the present work, the avalanche initiation problem has been studied assuming snow to be a continuum with a crack, as done by McClung[4]. It is the propagation of this crack, which leads to avalanche initiation. It is to be realised that the crack can propagate both by failure of snow in the weak layer and also due to interfacial bond failure between the weak and the strong layer. This interfacial failure can be quite prominent as bond development between the weak layer (of TG grains or frozen ice) and strong layer is quite poor. Data are not available for this interfacial strength and Bader and Salm[5] do not seem to have looked at this failure mode.

2. GOVERNING EQUATIONS

Though the snow slab is made of a number of weak and strong layers, it has been idealised as a continuum made of two strong layers with a weak layer sandwiched between these. The weak layer has a super-weak zone, which acts as stress concentrator. Fig.1 shows one such snow slab 20 m long, with 1 m thick strong layers and 5 mm thick weak layer. The crack region is 4 m long and the slab is lying on a uniform slope of 30°.

To determine the stress state in this slab, the following equations are needed for any layer:

Equilibrium Equation

$$\sigma_{ij,j} + \rho F_i = 0$$

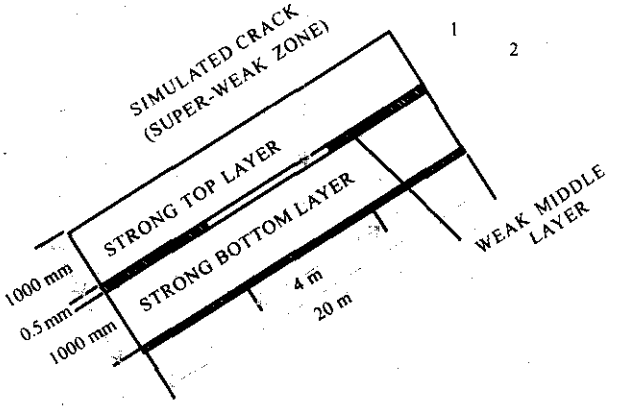

Figure 1. Structure of the snow slab model

Strain Displacement and Constitute Relation

$$\varepsilon_{ij} = \varepsilon_{ij}^e + \varepsilon_{ij}^c = \frac{1}{2}\left(\frac{\partial u_i}{\partial x_j} + \frac{\partial u_j}{\partial x_i}\right)$$

$$\dot{\varepsilon}_{ij}^c = \eta\left[\sigma_{ij} + \frac{\sigma_{kk}}{6}\delta_{ij}\right]$$

$$\varepsilon_{ij}^e = \frac{1+\nu}{E}\sigma_{ij} - \frac{\nu}{E}\sigma_{kk}\delta_{ij}$$

where

σ_{ij}	Stress
ρ	Density
F_i	Body force component
ε_{ij}	Total strain
ε_{ij}^e	Elastic strain
ε_{ij}^c	Creep strain
u_i, u_j	Displacement components
$\dot{\varepsilon}_{ij}^c$	Creep strain rate
η	Coefficient of viscosity
ν	Poisson's ratio
E	Modulus of elasticity
δ_{ij}	Kronecker delta

Boundary Conditions

The weak layer has a crack of varying length (1–10 m) and thickness of same magnitude as the thickness of the weak layer. The top layer is traction free. The bottom layer is assumed to be fixed to the ground, so that displacements due to gliding are neglected.

Material Properties

Physical Properties of all the three layers of the snowpack are listed below in Table 1.

Table 1. Physical properties of the top, middle, and the bottom layers of snowpack

	Top layer	Middle layer	Bottom layer
Density (kg/m³)	300	100	300
Thickness (m)	1.00	0.05	1.00
Length (m)	20	20	20
Poisson's ratio	0.3	0.3	0.3
Elastic modulus (N/m²)	10^9	10^8	10^9
Viscosity (Pa-s)	5×10^{10}	10^8	5×10^{10}

Failure Criterion

The propagation of the crack takes place by debonding along the interface of the layers or/and by fracture of snow particles. For the crack to propagate, two failure criteria one for failure of snow and the other for debonding between the layers are introduced. If the snow failure criterion is satisfied by a region, then the stiffness of that region is reduced to a very small value. Similarly, if the debonding criterion is met at a point of the interface, then the interface is separated into two surfaces at that point.

The failure criterion used for snow is one given by Narita[7] on the basis of tension tests. The failure strain for snow as shown in Fig. 2 is a function of strain rate. At strain rate of 10^{-3}, snow behaves as a brittle material.

Debonding is a process by which one can separate two initially and partially bonded surfaces under adequate loading condition.

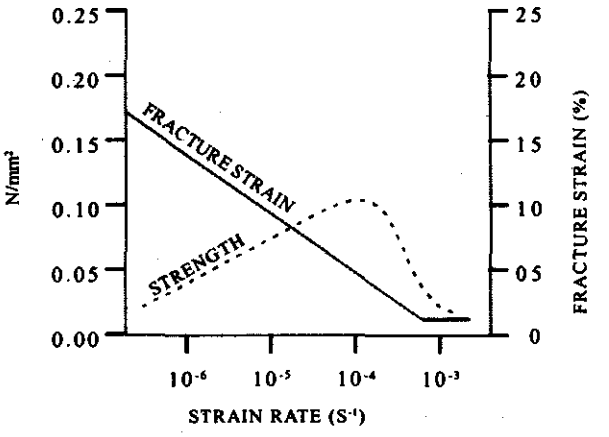

Figure 2. Plot of Narita for evaluation of fracture strain

The debonding criterion used in this model is

$$f = \sqrt{\left(\frac{\sigma_n}{\sigma^f}\right)^2 + \left(\frac{\tau_1}{\tau_1^f}\right)^2}, \quad \sigma_n = \max(\sigma_n, 0)$$

where

f	Fracture criterion
σ_n	Normal component of stress carried across the interface at the distance specied
τ_1	Shear stress components in the interface
σ^f and τ_1^f	Normal and shear failure stresses

If $f \geq 1$, the interfaces are assumed to have debonded.

2.1 Finite-element Modelling

To solve the above equations, finite-element method has been employed using a general purpose high ended package ABAQUS (version 6.2). Two-dimensional 4-noded quadrilateral and 3-noded triangular elements have been used. The triangular elements are mainly used at the crack tip. The model has around 14663 elements and 16025 nodes. Close to the crack tip the mesh is very fine and approximate area of element is 0.02 mm². whereas close to the free surface, it is about 10^5 mm². This grading of the mesh is achieved using multi-point

Figure 3(a). Full-mesh structure of the model

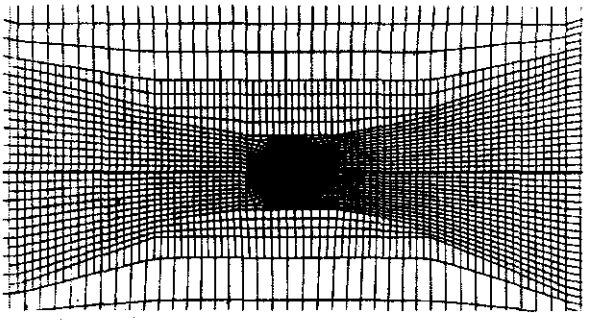

Figure 3(b). Zoomed portion of the left side dense region of Fig. 3(a).

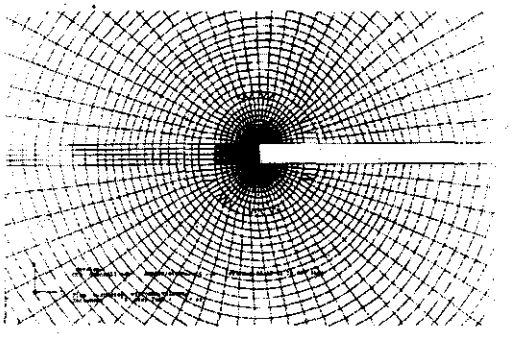

Figure 3(c). Zoomed portion of Fig. 3(b) exposing the left side crack tip.

constraint option available in ABAQUS. The fine grading of the mesh avoids numerical difficulties and convergence problems faced close to the crack tip under shear and compressive loads. Figure 3(a) shows the complete mesh along with exploded view of the mesh in Fig. 3(b) and Fig. 3(c) shows the fine grading close to the crack tip.

To model the compressible creep behaviour of snow, USER SUBROUTINE of ABAQUS was used to link the constitutive behaviour with ABAQUS. The deformation of snow under its own weight was studied for a load application time of 36 h. The crack propagation due to failure of snow and debonding between the layers (using the two failure criteria mentioned earlier) was observed during the load application. Both the failure criteria were applied simultaneously. The debond criterion is applied at the left-top corner and the bottom-right corner of the crack as shear stresses are maximum in these regions.

To analyse the debonding, a contact pair between the two crack surfaces was established to avoid penetration between these during the deformation. Contact was also established between the two surfaces ahead of the crack tip where the debonding phenomenon was to be carried out. To carry out the above phenomenon, duplicate nodes wereintroduced along the surface of the debond (i.e., at the same coordinate points) to facilitate the separation of the nodes under the debonding effect.

3. RESULTS & DISCUSSION

In the study of avalanche initiation stresses, σ_{12} and σ_{11} play an important role. σ_{12} seems to be responsible for the initial fracture of slab due to debonding subsequently, σ_{11} at the top corner of the crack and at the free surface of slab above the top corner seems to be responsible for breaking of slab from the remaining snow mass.

3.1 Stress Contours

Figure 4 demonstrates the distribution of shear stress contours σ_{12}, without the action of any load on the surface of the snowpack, along the left side top crack tip.

As stated, shear failure followed by tensile failure is the main reason of slab avalanche initiation. Thus, the σ_{11} contours in Fig. 5 show the likely spots of tensile failure, which would give a clear picture about the region, where tensile failure would occur. The limit of tensile strength for this plot is from +1.04e-03 to +1.719e-02 N/mm^2.

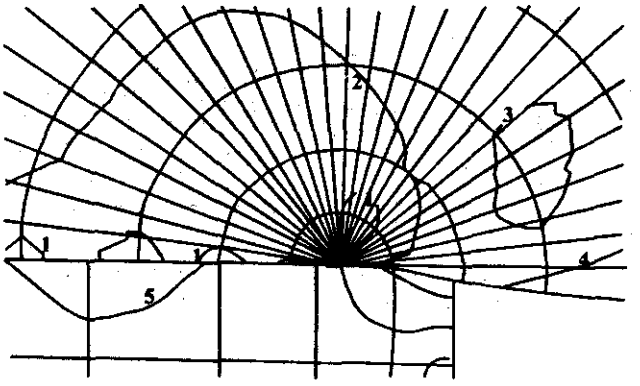

Figure 4. Contour plot for σ_{12} around the left side top crack tip. σ_{12} limits at 1 & 2 = + 3.867e-03 to + 2.802e-02 N/mm². σ^{12} limits at 3,4 & 5 = - 2.834e - 02 to -4.185e - 03 N/mm².

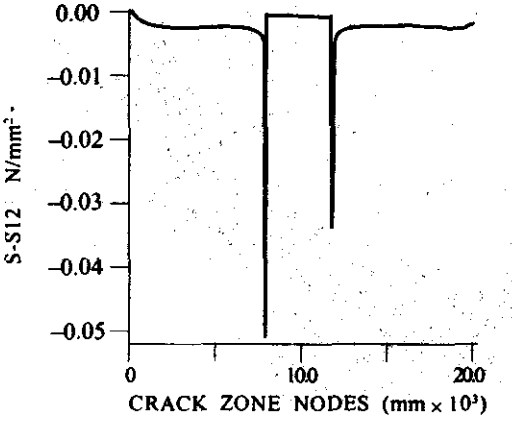

Figure 6. Plot of S12 along the interface between top and weak middle layers.

The distribution of shear traction between the top and weak layer interface has also been shown in graphical form in Fig. 6. The figure shows high stresses at the crack tip which fall down rapidly to 0.002N/mm² away from the tip. Figures 7(a) and 7(b) depict those elements ahead of the crack tip where strain in snow exceed the failure strain. For further analysis, the stiffness of these elements was reduced to zero. It was observed that very few elements in the slab exhibited this type of failure, as strain rates in those elements remained very low. The approximate size of this region is 1.2002m × 0.625m.

The debond crack propagates much faster down the slope, between the upper strong and the middle weak layer, as compared to other probable debond locations. This is shown schematically in Figs 8(a) and 8(b). The second mode of failure, debonding, seems to be more significant.

Various conditions can have an effect on the propagation of crack in a snowpack. Some of these conditions include crack length, bond strength between the interface layers, additional load due to weight of additional fresh snowfall. Following are some of the case studies that briefly elucidate the results

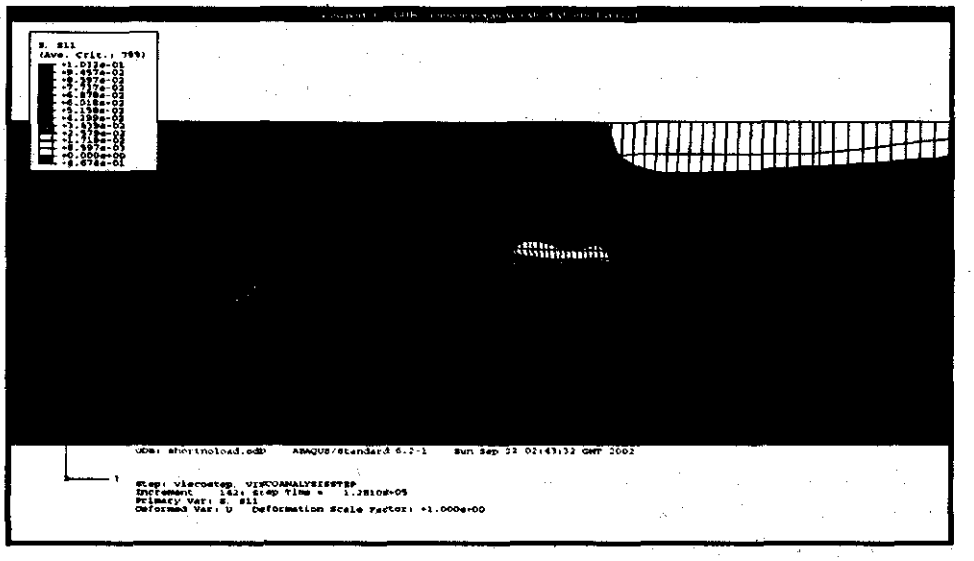

Figure 5. Region with white spots in the mesh indicating the highly tensile regions. σ_{11} limits at tensile regions = + 1.04e -03 to +1.719e -02 N/mm².

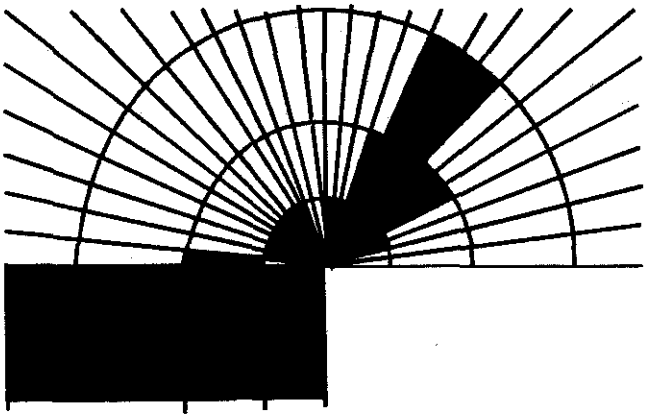

Figure 7(a). Highlighted portion of the failed elements at the left side top corner of the crack tip under application of damage criterion.

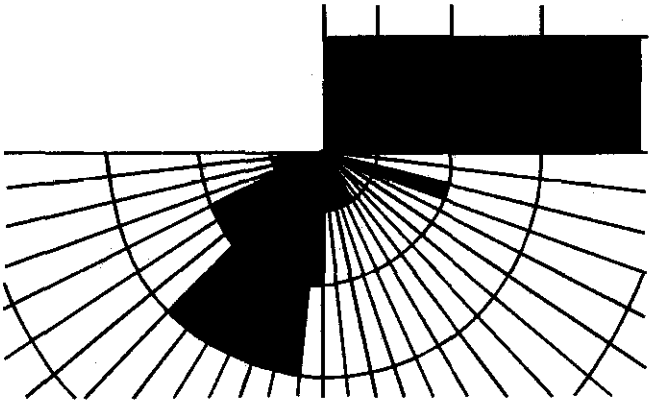

Figure 7(b). Highlighted portion of the failed elements at the right side bottom corner of the crack tip under application of damage criterion.

obtained for the debonding phenomenon in the snowpack under the influence of various parameters stated above.

3.1.1 *Case* 1

In this case, the effect of the weight of the additional fresh snowfall has been studied with some specified set of data shown in Table 2. To study the effect of this parameter, a snowpack model with a crack length of 4 m is taken.

Table 2 lists the result of debonding criterion with and without fresh snowfall load application on the snowpack with 4 m crack. To apply the debonding criterion for more length, one needs to have a finer mesh completely around the debond path. But the

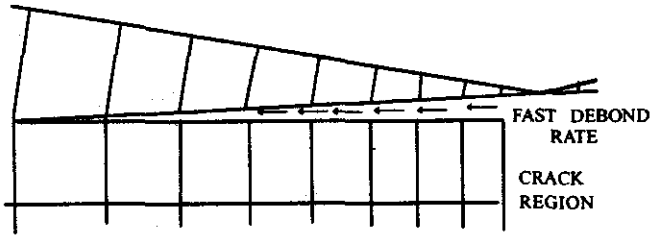

Figure 8(a). Region ahead of the crack tip at the left side top end debonding at a faster rate.

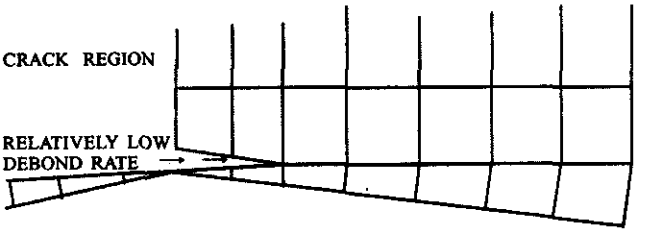

Figure 8(b). Region ahead of the crack tip at the right side bottom end debonding at a relatively slower rate.

mesh patterns in the present case are very fine at the crack tip and gradually coarsen towards the exterior areas. Thus, the study was limited to a debonding length of only 27 mm for the analysis with the first 20 nodes considered for debonding.

It can be observed from Table 2 that additional load due to fresh snowfall increases the rate of debonding.

Once the significance of debonding in snow failure was understood, the emphasis was on how debond strength between layers and additional loads on snow due to weight of snow or additional snowfall affect the rate of debonding. It may be mentioned

Table 2. Effect of skier load on debond time

Normal failure stress (N/mm^2)	Shear failure stress (N/mm^2)	Skier loading (N)	Debond time (s)
0.03	0.06	–	790.00
0.03	0.06	50	62.00
0.03	0.06	100	56.80
0.03	0.06	150	46.50
0.03	0.06	250	28.08

that no data are available for bond strength of snow and some representative bond shear strength values were taken. The bond normal strength values are not important as the interface experiences compressive loading.

3.1.2 *Case* 2

In this case the effect of crack length in a snowpack has been studied. For this analysis, models with the crack length of both 2 m and 4 m have been considered for better comparison. Initially, the models were analysed without the application of any surface load. Table 3 shows the results obtained from this analysis and gives a comparision of the effect of initial crack length on crack propagation time. It is observed that crack propagates to a longer length when the initial crack size is big. Also, the time taken for debonding 2.7 mm for 2 m crack length is 4254 s and is relatively more when compared with time required for 4 m crack length. Also in both the cases, debonding stopped very soon although deformation continued for the full 36 h.

Table 3. Shows the comparison of the effect of initial crack length on crack propagation time

Crack length (m)	Normal failure stress (N/mm^2)	Shear failure stress (N/mm^2)	No. of nodes debonded	Debond time (s)
2	0.03	0.1	5 (2.7mm)	4254
4	0.03	0.1	34 (64.5mm)	6740

Finally, debonding rates under 500 N external load for two different crack lengths were looked at. As the debonding phenomenon occurs at a very fast rate under the application of load, a debonding length of 102.5 mm with 43 nodes was considered for debonding in this analysis. The results from this analysis are presented in Table 4.

Thus, one could infer from Tables 3 and 4 that debonding rate is faster when the crack length is more and is relatively slower when the crack length is less.

Table 4. Effect of initial crack length on debond time with skier load of 500 N

Crack length (m)	Normal failure stress (N/mm^2)	Shear failure stress (N/mm^2)	Debond time (s)
2	0.03	0.1	97.0
4	0.03	0.1	73.5

4. CONCLUSION

It has been observed that the debonding rate in any snowpack with a crack in its weak zone is chiefly dependent on the crack length and weight of additional fresh snowfall or skier load. It can also be infered from this study that the failure in any snowpack is mainly due to debonding (i.e., interfacial failure) and not due to the failure of internal snow particles. Thus from this study one can conclude that an avalanche will be initiated primarily in an snowpack due to the presence of cracks in weak zones usually accompanied by an initial debonding.

REFERENCES

1. Perla, R. Slab avalanche measurements. *Can. Geotech. J.*, 1977, **1492**, 206-13.

2. Lachapelle, E.R. *et al.* Alternate methods of avalanche control. Washington State Highway Dept Res. Rep. 19.1. Olympia, *WA.*, 1975, 158 p.

3. Schweizer, J. Laboratory experiments on shear failure of snow. *Annals of Glaciology,* 1988, **26**, 97-102.

4. McClung, D.M. Direct simple shear tests on snow and their relation to slab avalanche formation. *Journal of Glaciology,* 1977, **19**(81), 101-09.

5. Bader, H.P. & Salm, B. On the mechanics of snow slab release. *Cold. Reg. Sci. Technol.*, 1990, **17**(3), 287-300.

6. Palmer, A.G. & Rice, J.R. The growth of slip surfaces in the progressive failure of over consolidated clay. *Proceedings of the Royal*

Society of London Scr. A, 1973, **332**(1591), 527, 518.

7. Narita, H. Mechanical behaviour and structure of snow under uniaxial tensile stress. *Journal of Glaciology,* 1980, **26** (94), 275-82.

8. K.A.S. Hibbit Inc., ABAQUS : Theory and Users' manuals, Version 6.2.

Contributors

Mr S Senthil obtained his BTech (Mech Engg) from the Universityof Madras, in 1999. Currently, he is employed as Project Staff at the Indian Institute of Technology Delhi. His areas of research include: Snow avalanche initiation mechanism using finite-element approach. His other areas of research include: Finite-element methods and analysis, snow mechanics, and fracture mechanics.

Dr P Mahajan obtained his PhD (Mech Engg) in 1990. Presently, he is working as Associate Professor in the Dept of Applied Mechanics at the Indian Institute of Technology Delhi. His research interests include: Composites, vibration, snow mechanics, fracture and application of finite-element method to above areas.